Proceedings of the 30th International Cosmic Ray Conference
Rogelio Caballero, Juan Carlos D'Olivo, Gustavo Medina-Tanco,
Lukas Nellen, Federico A. Sánchez, José F. Valdés-Galicia (eds.)
Universidad Nacional Autónoma de México,
Mexico City, Mexico, 2008
Vol. 1 (SH), pages 147–150

30TH INTERNATIONAL COSMIC RAY CONFERENCE

Travel delays of impulsive SEPs due to turbulent lengthening of magnetic field lines

B. R. RAGOT[1], S. W. KAHLER[2].
[1]*Helio Research, P.O. Box 1414, Nashua, NH, 03061 USA*
[2]*Air Force Research Laboratory/VSBXS, 29 Randolph Rd., Hanscom AFB, MA 01731 USA*

Abstract: The assumption that the first arriving particles in impulsive solar energetic particle (SEP) events travel scatter-free along regular Parker-spiral magnetic field lines from injection at the Sun to detection at 1 AU has led to the conclusion that the impulsive SEPs are usually injected well after a flare type III radio burst is observed at the Sun. If all the turbulent scales are taken into account in the description of the solar wind magnetic fields, however, one finds that the lengths of the field lines, and therefore the path lengths of the SEPs, are much increased by the turbulence. Close to 1 AU, the length of a turbulent field segment is increased on average by close to 50%, with even longer field lines in some slow SW streams. In impulsive SEP events, noticeable travel delays of the first arriving particles should result from this turbulent lengthening of the field lines, with significant variations of these travel delays from one event to another. We argue that the delays of the particles occur during their travel to 1 AU, mostly close to 1 AU, not at their injections at the Sun. Particles with lower energies and smaller gyroradii may undergo longer trajectories and larger travel delays than do higher energy particles.

Introduction

An important aspect of solar energetic particles (SEPs) is to determine their acceleration and injection profiles at the Sun. It has long been assumed that the first observed SEPs of all energies of transient events at 1 AU arrive after traversing common spiral field lines over distances of 1.2 AU with little scattering (e.g., [1]). The SEP onsets show the velocity dispersions expected from impulsive releases at the Sun of particles of all observed energies. The standard technique to deduce the onsets of SEP solar injection times is to plot the times of the first arriving particles (T_0) against c/v where v is the speed of the particles (e.g., [2]). The intercept of the plot at the time axis gives the inferred solar onset time of injection.

The use of c/v plots and scatter-free assumption for first arriving particles has recently produced puzzling results. Although it had long been accepted that solar $E \geq 30$ keV electrons were injected in type III radio bursts [3] of the flare impulsive phase, recent observations from the *ACE* EPAM (e.g., [4]) and *Wind* 3DP [5] spacecraft detectors have indicated coronal injection onsets delayed by ~ 10 minutes from the type III bursts. A recent comparison [6] of inferred injection times of 80 E $\geq$ 30 keV electron events with solar 40-800 MHz observations found no single kind of solar radio signature, other than the preceding type III bursts, to characterize the inferred electron injection onset times. Inferred injection times of electrons and ions in gradual SEP events at 1 AU [2] are inconsistent among different events and with the earlier *Helios* events observed well within 1 AU. Furthermore, the c/v plots have generally yielded simultaneous ion and electron injections in impulsive SEP events [2], but delayed relative to the type III bursts, contrary to the earlier *ISEE-3* [7] and *Helios* [8] observations.

Simulations [9, 10] with various assumptions of scattering have shown that, although the particle onset times usually align close to a straight line as a function of c/v, the estimated injection times and path lengths can deviate significantly from actual values. We review a major effect not considered in those simulations, that turbulence results in magnetic field-line wandering to produce field-line lengths substantially longer than 1.2 AU [11].

Turbulent Lengthening

The SEP path lengths cannot be less than the length of the field lines resolved at the scale of a few of their gyroradii, as the particles are forced to follow the irregularities of the field lines down to those scales of a few gyroradii. The gyroradii of SEPs are orders of magnitude shorter than 1 AU and, thus, to evaluate a lower limit for the SEP path lengths, one must describe the turbulent field lines of the SW over a very broad range of turbulent scales. This can be done using the spectra of magnetic turbulence measured *in situ*.

Applying the SRND method [12, 13] with magnetic spectra deduced from *Helios 2* magnetic field measurements at 1 and 0.3 AU in quiet slow and fast SW streams, we computed 50 three-dimensional magnetic field lines in each of the SW turbulence conditions. Each of the magnetic field lines has a projection along the main field of about 4×10^{12} cm. Figure 1 shows examples of these magnetic field segments projected in the $x - z$ plane of the ecliptic. Of the four cases showing the field-line wandering on the relatively large scales of $10^{10} - 10^{12}$ cm, slow SW at 1.0 AU contains the lowest power in the short ($10^{10} - 10^{11}$ cm) turbulent scales, while fast SW at 0.3 AU contains the highest power in those same short scales. This results in the smoothest field line in the first case and the most irregular field line in the second. Slow SW at 0.3 AU and fast SW at 1.0 AU are intermediate between the two.

We then computed the length $L_{\delta z}$ of each of the field lines as a function of the resolution scale, δz, between 10^9 and 10^{12} cm. The results of all 200 computations are shown in Figure 2, rescaled by the projected length $\Delta z = 4 \times 10^{12}$ cm. The histograms of the ratios $L_{\delta z}/\Delta z$, or lengthening factors, at resolution 10^9 cm are also shown in Figure 3. The ratio $L_{\delta z}/\Delta z$ is the correction factor that should be applied to the length of a field-line segment's smooth approximation in order to obtain the length of the real turbulent field-line segment seen at the resolution δz. Here the smooth approximation is just the projection Δz along the main field.

The lengthening factor $L_{\delta z}/\Delta z$ can be very significant. It varies from about 1.16 ± 0.06 and 1.23 ± 0.03 in slow and fast SW at 0.3 AU to 1.45 ± 0.25 and 1.33 ± 0.06 in slow and fast SW at

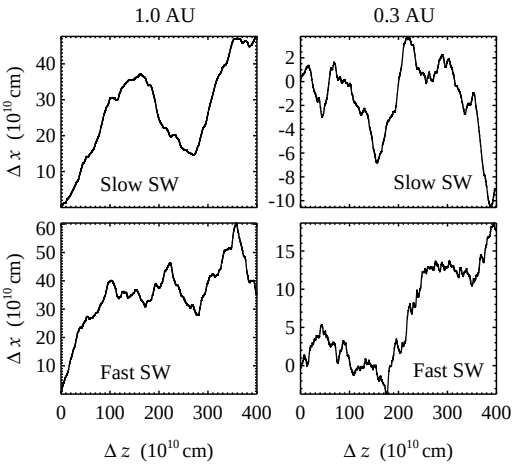

Figure 1: Examples of projected magnetic field-line segments generated from 3D isotropic turbulence spectra composed of some 10^{15} modes, with the projected B_x spectral fits of Fig 2 in [13].

1 AU, with a few more extreme values. The variations from one SW stream to another SW stream with the same turbulence spectrum but different turbulent phases is mainly due to the large-scale field-line wandering. As the resolution scale δz becomes finer and more short-scale irregularities are accounted for in the computation of the length $L_{\delta z}$, the curves of the correction factors in different realizations of the turbulence increase nearly parallel to each other, due to the independence of the scales and the higher statistics on the shorter turbulent scales.

The correction $L_{\delta z}/\Delta z$ increases with distance from the Sun because the decrease in r^{-4} of B_0^2 is faster than that of the magnetic turbulent energy, implying a stronger field-line wandering at larger distance from the Sun in the inner heliosphere. Also, the dependence of the lengthening factor on δz is stronger in the fast SW where the turbulence has less time to evolve and the spectra are flatter, implying more short-scale irregularities along the field lines (see Fig. 1).

Applying the generalized quasilinear (GQL) theory [14, 12], whose accuracy in quiet SW was confirmed by a full nonlinear calculation [15], we can also predict the average lengthening of the turbulent field lines, analytically, at any resolution scale.

$$\langle L_{\Delta z,\delta z} \rangle = \frac{\Delta z}{\delta z} \langle \left[(\delta z)^2 + (\delta r)^2_{\delta z} \right]^{1/2} \rangle \ , \qquad (1)$$

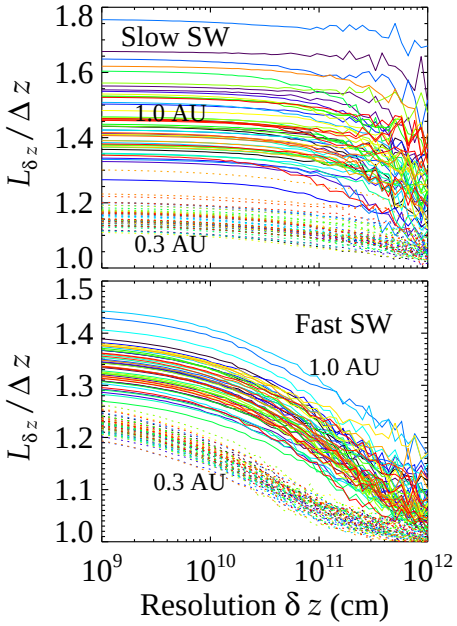

Figure 2: Ratio $L/\Delta z$, or field-line lengthening factor, as function of the resolution scale δz. The lengths of the wandering field lines vary from one SW stream to another, even for a fixed spectrum of turbulence. Variability is stronger in slow SW where, unlike in fast SW, wandering on a 0.1 AU ($\sim 10^{12}$ cm) scale can produce as much lengthening as irregularities on the shorter scales.

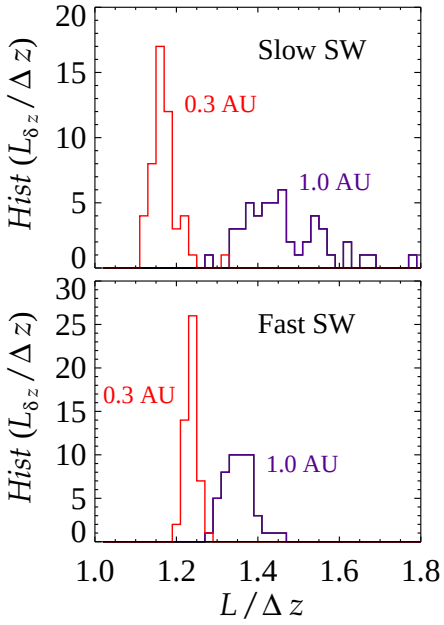

Figure 3: Histograms of the ratios $L/\Delta z$ of Fig. 1 at resolution $\delta z = 10^9$ cm.

where $(\delta r)^2_{\delta z} = (\delta x)^2_{\delta z} + (\delta y)^2_{\delta z}$ is distributed according to the distribution (see § 4.1 in [13])

$$Prob\{(\delta r)_{\delta z} = X\} = \frac{2X}{\sigma^2} e^{-X^2/\sigma^2} \qquad (2)$$

and $\sigma^2 = \langle (\delta r)^2_{\delta z} \rangle$ is related to the turbulence spectrum through the GQL theory. Provided that $2\pi/\delta z$ exceeds the correlation wavenumber k_{cor} of the turbulent phases and for a system sufficiently large in all directions, it can be shown that the cross-field displacements δx and δy are random numbers drawn from the Gaussian distribution $f_X(\delta x) = \pi^{-1/2}\sigma^{-1}e^{-(\delta x)^2/\sigma^2}$ (see [12]), and therefore, δr, is drawn from the distribution of eq. (2). Estimating the average we find

$$\frac{\langle L_{\Delta z,\delta z}\rangle}{\Delta z} = 1 + \frac{\pi^{1/2}}{2}\frac{\sigma}{\delta z}\left[1 - \Phi\left(\frac{\delta z}{\sigma}\right)\right] e^{(\delta z)^2/\sigma^2} \qquad (3)$$

with the error function Φ. We compare in Figure 4 the theoretical estimate of eq. (3) (*dash-dotted lines*) to the average of the 50 curves shown in each SW case in Figure 2 (*solid lines*). The discrepancy results from the difficulty to "deproject" the spectra with sufficient accuracy over 4 decades.

Figure 4 also shows the lengthening factors obtained from *Helios 2* data (*crosses with error bars*). Although slightly different in slow SW from the average values of simulation and theory, the values computed from the *in situ* data are, given the distributions of Figure 3, very close to the average. Because each of the data intervals selected for analysis is 4-5 times longer than one simulated field line, the results from the *in situ* analysis are much closer to the average values than would be expected from the distributions of Figure 3.

Travel Delays and Minimal Path Length

The lengthening factors shown in Figures 2-4 apply locally and for nearly uniform turbulence conditions. To estimate the length of turbulent field lines between the Sun and 1 AU, the field lines must be subdivided into a number of smaller segments. Four adjacent segments from the Sun to 0.2, 0.4, 0.7 and 1 AU are adequate. As reference

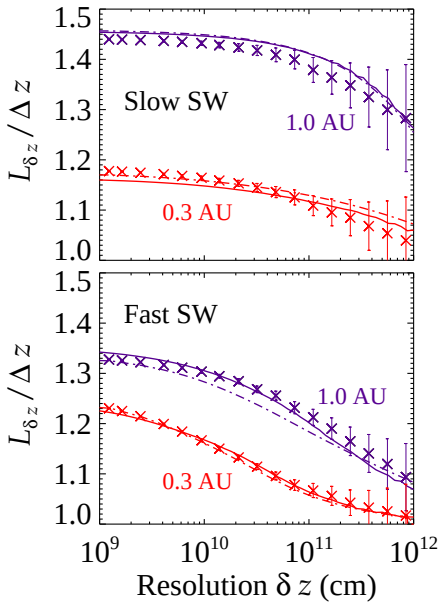

Figure 4: Ratios $L/\Delta z$ as function of δz, showing excellent agreement between simulation, theory and *in situ* observations. *Dash-dotted lines:* averages for 50 simulated field lines. *Solid lines:* theoretical estimates of the averages. *Crosses with error bars:* ratios computed from *Helios 2* data.

length we use for each of the four segments the length of the corresponding Parker spiral segment.

We find that in quiet slow SW, the length of the field lines exceeds, on the average, 1.5 AU between the Sun and 1 AU, with maxima as high as 2 AU and minima of the order of 1.2 AU. The resulting travel delay for an "unscattered" 10 MeV proton traveling from a few solar radii to 1 AU could exceed 23 ± 14 minutes in slow SW, 19 ± 4 minutes in fast SW (see details in [11]). The travel delays of "unscattered" 5 keV electrons with gyroradii $\leq$ a few 10^7 cm at 1 AU ($< 1/100$ that of 10 MeV protons) should be similar to those of the 10 MeV protons in slow SW, but even longer in fast SW. These results are very much consistent with the broadly distributed injection times of E $>$ 40 keV electrons obtained in [4].

To obtain a rough absolute lower limit of the field-line lengths, we also use as reference line the radial line with three adjacent segments of lengths 0.3, 0.5 and 0.2 AU, respectively, and as lengthening factors: 1, 1.1, 1.25 in slow SW and 1, 1.14 and 1.23 in fast SW (see Figs. 2-3). By doing so we find that in fast SW, the small-scale irregularities guarantee that $L_{\delta z} > L_{spiral}$ as soon as $\delta z \leq 10^{10}$ cm. In slow SW, $L_{\delta z} > 1.1$ AU for $\delta z \leq 10^{10}$ cm. A higher lower limit in excess of L_{spiral} could easily be found by refining our estimate to a fourth intermediate segment between 0.5 and 0.8 AU. So, field-line wandering may not explain SEP path lengths shorter than L_{spiral}, contrary to the conclusion reached in [16] where the shorter turbulent scales, responsible for the minimal turbulent lengthening, were not taken into account.

Finally, the travel delays are shorter for faster particles, and longer for slower particles, since they are proportional to the travel time, and the lengthening factors $L_{\delta z}/\Delta z$ are decreasing functions of the particle gyroradius. The variations are only of the order of 10% in quiet SW between particles with 10^{10} and 10^{11} cm gyroradii, but they could become much more significant for enhanced levels of SW turbulence.

References

[1] Haggerty, D. K., and E. C. Roelof. *Astrophys. J.*, 579, 841, 2002.
[2] Kahler, S., and B. R. Ragot. *Astrophys. J.*, 646, 634, 2006.
[3] Lin, R. P. *Solar Phys.*, 100, 537, 1985.
[4] Haggerty, D. K., E. C. Roelof, and G. M. Simnett. *Adv. Space Res.*, 32, 2673, 2003.
[5] Klein, K.-L., S. Krucker, G. Trottet, and S. Hoang. *Astron. Astrophys.*, 431, 1047, 2005.
[6] Kahler, S. W., H. Aurass, G. Mann, and A. Klassen. *Astrophys. J.*, 656, 567, 2007.
[7] Reames, D. V., T. T. von Rosenvinge, and R. P. Lin. *Astrophys. J.*, 292, 716, 1985.
[8] Kallenrode, M.-B., and G. Wibberenz. *Astrophys. J.*, 376, 787, 1991.
[9] Lintunen, J., and R. Vainio. *Astron. Astrophys.*, 420, 343, 2004.
[10] Sáiz, A., P. Evenson, D. Ruffolo, and J. W. Bieber. *Astrophys. J.*, 626, 1131, 2005.
[11] Ragot, B. R. *Astrophys. J.*, 653, 1493, 2006.
[12] Ragot, B. R. *Astrophys. J.*, 645, 1169, 2006.
[13] Ragot, B. R. *Astrophys. J.*, 651, 1209, 2006.
[14] Ragot, B. R. *Astrophys. J.*, 525, 524, 1999.
[15] Ragot, B. R. *Astrophys. J.*, 644, 622, 2006.
[16] Pei, C., Jokipii, J. R., & Giacalone, J. 2006, ApJ, 641, 1222.